Archival Report

Biological Psychiatry: GOS

The Nonclassic Psychedelic Ibogaine Disrupts Cognitive Maps

Victorita E. Ivan, David P. Tomàs-Cuesta, Ingrid M. Esteves, Davor Curic, Majid Mohajerani, Bruce L. McNaughton, Joern Davidsen, and Aaron J. Gruber

ABSTRACT

BACKGROUND: The ability of psychedelic compounds to profoundly alter mental function has been long known, but the underlying changes in cellular-level information encoding remain poorly understood.

METHODS: We used two-photon microscopy to record from the retrosplenial cortex in head-fixed mice running on a treadmill before and after injection of the nonclassic psychedelic ibogaine (40 mg/kg intraperitoneally).

RESULTS: We found that the cognitive map, formed by the representation of position encoded by ensembles of individual neurons in the retrosplenial cortex, was destabilized by ibogaine when mice had to infer position between tactile landmarks. This corresponded with increased neural activity rates, loss of correlation structure, and increased responses to cues. Ibogaine had surprisingly little effect on the size-frequency distribution of network activity events, suggesting that signal propagation within the retrosplenial cortex was largely unaffected.

CONCLUSIONS: Taken together, these data support proposals that compounds with psychedelic properties disrupt representations that are important for constraining neocortical activity, thereby increasing the entropy of neural signaling. Furthermore, the loss of expected position encoding between landmarks recapitulated effects of hippocampal impairment, suggesting that disruption of cognitive maps or other hippocampal processing may be a contributing mechanism of discoordinated neocortical activity in psychedelic states.

https://doi.org/10.1016/j.bpsgos.2023.07.008

The retrosplenial cortex (RSC) is well positioned to integrate sensory, mnemonic, motivational, and cognitive information by virtue of its strong connectivity with the hippocampus (1), medial prefrontal cortex (2), and primary sensory cortices (3,4). The normal covariation of activity among these structures revealed by functional magnetic resonance imaging in humans is disrupted by classic psychedelics such as lysergic acid diethylamide and psilocybin (5,6). Here, we tested whether coordination of activity among individual neurons within the RSC is disrupted and how this affects the encoding of information.

Many neurons in the rodent RSC encode spatial position (7). In head-fixed mice, such RSC neurons encode the virtual position of the animal on a treadmill by activating reliably at specific belt positions (8). Therefore, these neurons have signaling properties similar to the place cells in the hippocampus, which seem to represent a cognitive map of space (9,10) and may provide a contextual/index code to bind together attributes of experience that are represented in the neocortex (11,12). The current position of an animal is encoded by the activity state of place cells comprising the cognitive map for a given environment. As an animal locomotes, it uses an estimate of the distance and direction of movement to update the ensemble activity according to the cognitive map to reflect the new expected position (13). This process is called path integration. Animals can correct for accumulated errors of path integration when familiar landmarks are encountered (14).

Head-fixed mice running on a treadmill belt are able to engage these systems. In this preparation, RSC place cells have activity that is stable over multiple laps of the belt, even in the absence of landmarks other than a start location (8). This suggests that head-fixed mice are capable of using path integration to update the cognitive map to infer the virtual position on a treadmill belt. Both the RSC and hippocampus seem to be involved in this process. Inactivation of the hippocampus disrupts RSC place cell stability (15), and RSC inactivation impairs path integration in freely moving animals (16). Regardless of the relative roles of these structures in the underlying computations, the positional signal in the RSC provides a window into the brain's ability to maintain a cognitive map and update it appropriately to infer position between landmarks. Here, we tested the effects of ibogaine on the encoding of positional inference and the associated coordination of neural firing in the RSC to test the theory that drugs with psychedelic effects disrupt the brain's ability to generate predictions and regulate neural activity (17).

Ibogaine evokes mental states with psychedelic features in humans (18). It is considered a nonclassic psychedelic because it has significantly broader neuropharmacological action than classic psychedelics (19). Nonetheless, both classes affect phenomena linked to cognitive maps, including

ISSN: 2667-1743

navigation (20,21) and mood disorders (22–24). The current work focuses on navigation because it is much better understood than mood regulation in animal models.

METHODS AND MATERIALS

Animals

Adult (9- to 11-month-old) Thy1-GCaMP6m mice (N = 8; 3 female/5 male) weighing 30 to 35 g were housed in standard rodent cages and maintained at 24 °C under a 12-hour light/dark cycle. Mice had free access to food and water before training. All experiments were performed during the light cycle (between 7:30 AM and 7:30 PM). Procedures were in accordance with the guidelines established by the Canadian Council on Animal Care, and protocols were approved by the Animal Welfare Committee of the University of Lethbridge.

Surgery

Mice received a 5-mm bilateral craniotomy (anteroposterior: +1 to −4; mediolateral: −2.5 to +2.5), which was then covered with a coverslip, and a titanium head plate was fixed to the skull for head fixation. Full description of the surgical procedure can be found in Supplemental Methods.

Drugs

Ibogaine HCl was obtained from Toronto Research Chemicals, Canada, in powder form and diluted in sterile water to a concentration of 10 to 12 mg/mL to achieve a dose of 40 mg/kg in a 0.1-mL volume for each mouse (intraperitoneal administration). This dose is based on previous reports (25–27). Our pilot studies had indicated that this concentration produced moderate levels of behavioral indicators typical of psychedelics (tremors, ataxia) while allowing animals to complete trials of the task. The control animals received 0.1-mL 0.9% saline solution. We chose saline instead of water for the control at the recommendation of the University's Animal Care Staff to minimize any potential issues with the intraperitoneal injections.

Experimental Procedure for Behavior

Head-fixed mice were trained to run on a treadmill using a positive reinforcement paradigm. They received a drop of 10% sucrose solution on every trial, which consisted of 1 lap of the treadmill belt. Animals were water restricted during the training and testing. They had ad libitum access to water for up to 30 minutes per day, and their body weight was carefully monitored throughout the experiment to ensure that the weight loss did not exceed 15% of their baseline weight. The treadmill belt consisted of a Velcro strip that was 150 cm long and 4 cm wide. Three tactile cues were placed in different locations on the belt. Licking behavior was recorded using a capacitive sensor that was connected to the lick spout. An optical encoder attached to the wheel shaft was used to monitor belt movement. A microcontroller was used to monitor the encoder, licking sensor, and reward delivery.

Neural activity was imaged in daily sessions of the task. There were 3 10-minute epochs of recording while mice performed the task, one before drug or saline and two afterward. This allowed us to control for day-to-day variance in performance and to test the effects of injections on a well-isolated population of neurons. The first 10-minute epoch in every session was the baseline condition before injection. Mice were then given an injection of ibogaine or saline and waited 10 minutes (while still head-fixed) for the drug to take effect. The second epoch of the task and recording began again for 10 minutes (minutes 20–30 of the experiment). The third 10-minute recording epoch began 30 minutes after injection. All analyses were performed at the 2 postinjection epochs independently. Remarkably, every analysis was consistent among these epochs. Therefore, for the sake of conciseness and to reduce the complexity of figures, we only present analysis of the first 10-minute epoch in the main text. The supplemental figures show data at both time points. Each animal was imaged in 1 session before receiving any injections (predrug day 1) for 2 days of saline injections and then either 3 days (test days 1–3) of ibogaine HCl (40 mg/kg; n = 6) or 3 days of saline (n = 2). The control group consisted of the 2 animals that received only saline and the initial injection of saline in the 6 animals that later received ibogaine, for a total of 18 sessions.

Neural Activity Analysis

A full description of the methods used for imaging, preprocessing, computing spatial encoding, decoding error, and unit functional connectivity along with the neuronal avalanche analysis methods are provided in Supplemental Methods.

RESULTS

We used two-photon imaging to record the activity of ensembles of individual RSC neurons (153–702 simultaneous cells per session) in head-fixed mice (Figure 1A). Mice were placed on a treadmill belt that had narrow tactile cues in 3 positions along its length. Mice received a liquid reward on every lap of the belt. A within-session design was used to test drug effects compared with baseline conditions in the same populations of neurons (Figure S1).

Ibogaine Disrupts Encoding of Inferred Position

Prior to any injections, some RSC cells activated at a specific position of the belt during each trial (Figure 1B). Other cells were not selective to position or were inconsistent from trial to trial. Therefore, we computed the adjusted mutual information (MI) between activity and belt position, which captures both sources of variance (28), to restrict analysis to those cells that were most selective to position. The injection of ibogaine (40 mg/kg, intraperitoneally) destabilized the place firing of these RSC cells and correspondingly led to a significant decrease in mean MI compared with baseline (Figure 1B and Figure S2.1) (paired t test, $t_{16} = 5.135$, $p = 9.978 \times 10^{-5}$). In contrast, there was a slight increase in mean MI following saline ($t_{10} = -2.86$, $p = .017$). The distribution of position fields among the population of high MI cells (top quartile) extended over the entire belt prior to injections (Figure 1C).

Next, we evaluated whether the RSC encoded a map of the virtual location on the belt, by testing whether the belt position at any moment could be decoded from ensemble RSC activity. Indeed, position was decodable with far less error than expected by chance (paired t test, $t_{27} = 11.724$, $p = 4.218 \times 10^{-12}$),

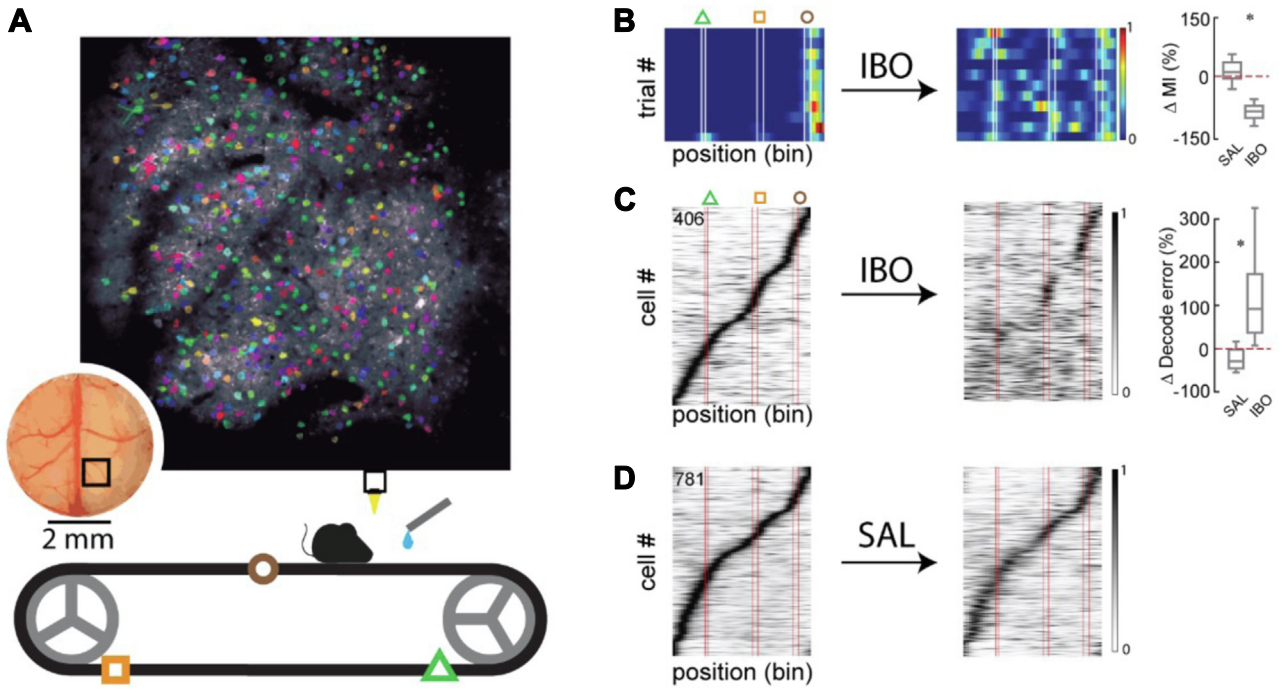

Figure 1. Ibogaine disrupts encoding of virtual position. **(A)** Illustration of experimental setup (bottom) and sample image showing segmented neurons (indicated by colored patches) within the field of view over the retrosplenial cortex (inset). Symbols on the treadmill belt indicate approximate locations of tactile cues. **(B)** Activity of 1 neuron as a function of position on the belt for several consecutive trials. Vertical lines indicate locations of tactile cues. The neuron selectively activates at one position prior to ibogaine but loses location specificity after injection. The right panel shows the change in session-averaged adjusted MI from baseline for all sessions (n = 17). **(C)** Session-averaged activity of position-tuned cells before (left panel) and after (center panel) injection of ibogaine for all sessions. Cells in both panels are ordered by a lag to peak activity before injection. The right panel shows the change in decoding error after injection of ibogaine. **(D)** The same as **(C)**, but for saline injection. *$p < .001$. IBO, ibogaine; MI, mutual information; SAL, saline.

consistent with previous reports (8). Ibogaine disrupted the map encoded by ensembles and led to significantly greater decoding error by a classifier trained on baseline data (Figure 1C and Figure S2.2) (paired t test, $t_{16} = -8.456$, $p = 2.683 \times 10^{-7}$), whereas saline did not (Figure 1D) (paired t test, $t_{10} = -0.23$, $p = .823$). Unsurprisingly, the increase in decoder error was proportional to the decrease in mean MI values (Figure S2.3). Interestingly, the disruption by ibogaine was more prominent in the ambiguous regions of the belt between the tactile cues. This is evident in the persistence of place fields by some cells at the cue regions (Figure 1C). We tested this by comparing the MI of cells responding at cue locations to the MI of cells responding at positions between the cues. A rank-order analysis of the top quartile of MI values in the 4 conditions (saline/ibogaine × cue/intercue) revealed a significant interaction of cue and ibogaine on MI (Kruskal-Wallis $t_7 = 235.978$, $p = 2.66 \times 10^{-47}$) (Figure S2.4). The MI values of cells were not different between cue and noncue locations prior to ibogaine (Nemenyi post hoc test $p = .355$), but there were more highly informative cells at cue locations than at noncue locations after ibogaine ($p = 3.34 \times 10^{-3}$). Saline did not produce this difference between cue and noncue locations ($p = .556$). Note that the MI of cue location cells did not decrease after ibogaine ($p = .265$), whereas the MI of noncue cells did decrease after ibogaine ($p = 1.44 \times 10^{-9}$). These results indicate that ibogaine impairs signaling of position more drastically at the ambiguous regions between cues when position estimates depend on path integration and cognitive maps. Despite the disruption of the cognitive map, mice continued to perform the task after ibogaine with only moderate decreases in movement velocity and other metrics (Figure S1). Finally, we tested whether a new map of space forms after ibogaine by training a new classifier on the postibogaine data. The error of this classifier tested on postibogaine data (cross-validated) was significantly higher than the error of the classifier that was trained and tested on baseline data prior to injection (paired t test, $t_{16} = -7.119$, $p = 2.436 \times 10^{-6}$), indicating that there had not been a remapping of position. Instead it seems that there was no stable mapping of noncue positions after ibogaine.

The mean activity rate during the task increased following ibogaine ($t_{16} = -5.112$, $p = 1.044 \times 10^{-4}$), but not saline ($t_{10} = 1.345$, $p = .208$). It has been proposed that sensory inputs become disinhibited under psychedelics (17), so we expected proportionally greater increases in firing rate during traverses of the tactile cue patches than at positions between the cues. Indeed, we found evidence to support this prediction. On the cells with the MI in the fourth quartile, we computed the ratio between the cue and noncue location activity of each cell. This ratio increased after ibogaine (paired t test, $t_{16} = -2.983$, $p = .009$), but not saline (paired t test, $t_{10} = -0.468$, $p = .65$). This indicates that the increased

activity was greater during cue traverses than during noncue regions of the belt.

Ibogaine Reduces Functional Connectivity

Studies with humans have shown that covariance of activity among brain regions is reorganized by psychedelic compounds to attenuate dominant motifs (29,30). Therefore, we tested whether a similar reorganization occurs at the cellular level. We computed the correlation of activity among all neurons recorded simultaneously during a session before injection and used hierarchical clustering to order the units so that functionally similar units were adjacent. This matrix defines the functional connectivity. We applied the same matrix ordering to the data that were collected after injection to be able to visualize changes in correlation structure. Injection of ibogaine drastically changed the correlation structure, whereas saline seemed to reduce the amplitude of correlations but preserve the overall pattern (Figure 2A, B). We quantified injection-related changes by computing the clustering coefficient of all pairwise correlations, which indicates how distinct clusters of correlated units are from one another (Figure 2C). Saline had no effect ($t_{10} = -0.794$, $p = .446$), but ibogaine significantly reduced the clustering coefficient (paired t test, $t_{16} = 6.477$, $p = 7.639 \times 10^{-6}$). This analysis of pairwise correlations indicates that the network has become functionally more homogeneous. Next, we investigated covariance among larger groups of cells using principal component analysis to decompose neural activity into a reduced space. During baseline sessions, the top 6 factors accounted for 72.9 ± 4.7% of the explained variance. After ibogaine administration, a new decomposition revealed that the explained variance of the top 6 factors dropped significantly to 64.8 ± 2.6% (Figure 2D and Figure S3) (repeated-measures analysis of variance [RM-ANOVA], Bonferroni's t test $t_{1,32} = 21.86$, $p = 5.096 \times 10^{-5}$). Saline did not have this effect (explained variance = 76.5 ± 4.1%; RM-ANOVA, Bonferroni's t test $t_{1,20} = 0.099$, $p = .755$). This indicates a significant reduction in the covariance of activity

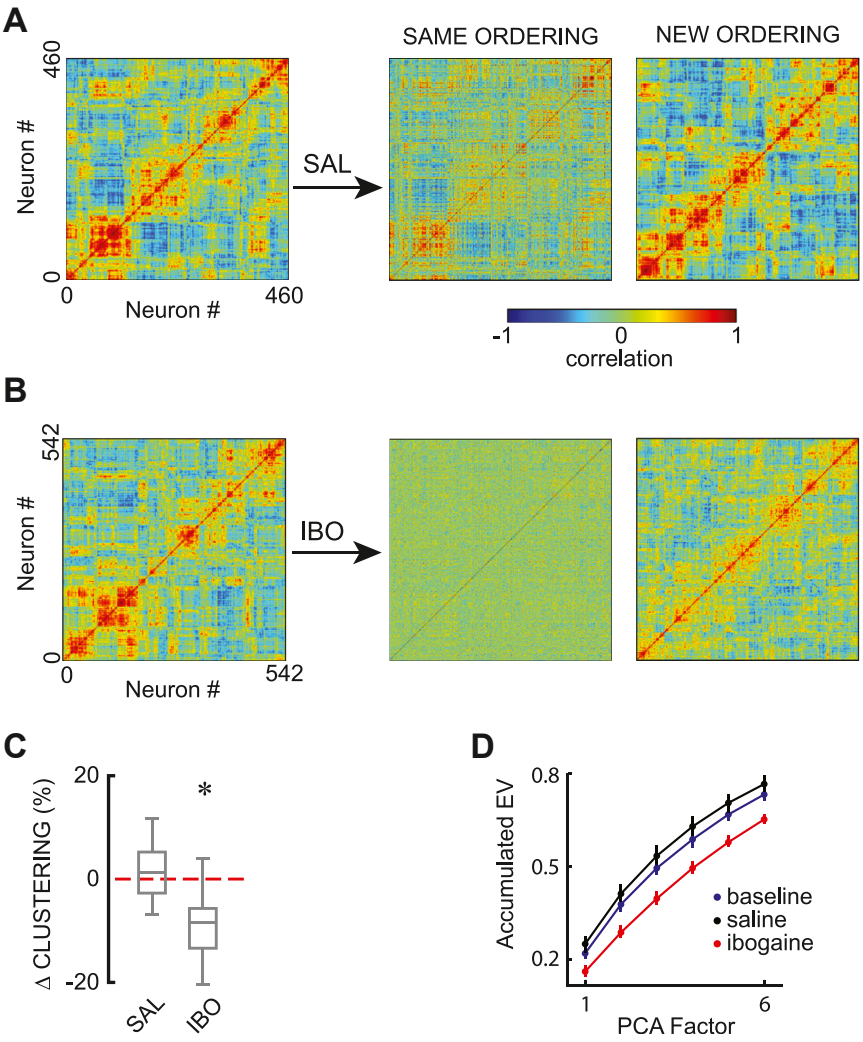

Figure 2. Population covariance. **(A)** Pairwise correlation of unit activity in 1 representative session prior to injection (left panel) and after saline injection. The middle panel has the same ordering as the left panel, and the right panel shows a reclustering of correlation patterns. **(B)** Pairwise correlation before and after injection of ibogaine in 1 session, showing that functional connectivity is reorganized and becomes less structured (fewer large blocks of high correlation) after injection. **(C)** Box plot of the change in clustering coefficient of the correlation matrices from baseline. The reduced clustering after ibogaine reflects a loss of dominant functional connectivity motifs. **(D)** Cumulative explained variance as a function of principal component factors, showing that signaling among neurons becomes more independent after ibogaine. *$p <$ .0001. EV, explained variance; IBO, ibogaine; PCA, principal component analysis; SAL, saline.

among groups of cells such that activity is more independent among units after ibogaine. These data suggest that functional connectivity is reduced after ibogaine administration.

Higher-Order Statistics

The loss of spatial information could arise from disruption of processing within the RSC or from disruption of structured input to the RSC, such as from the hippocampus. To shed light on which is more likely, we next sought to determine how ibogaine affected the propagation of signals within the RSC. One approach to quantifying such dynamics is to assess the size and duration of activity burst events in the network, which are often called information cascades or neuronal avalanches (31). The relationship between the size and duration follows power-law statistics (32,33), which are characteristic of physical systems that are near a critical state separating distinct dynamic regimes. It has been proposed that the brain is self-tuned to lie at the boundary between an ordered and disordered phase that supports self-sustained activity. Furthermore, recent functional magnetic resonance imaging data suggest that brain networks shift toward criticality (e.g., more disorganized) under psychedelics (34). Next, we tested whether ibogaine has a similar effect at the cellular level.

Avalanche events and quiescent periods between events were detected according to previous work (35) (Figure 3A; see Supplemental Methods). Briefly, activity was binned and summed across all units. Each excursion of summed activity over a threshold is a neural avalanche. The duration of the avalanche is the number of consecutive bins by which the summed activity exceeds the threshold, and the duration of quiescent periods is the time between the end of one avalanche and the start of the next one. The avalanche size is the area under the curve between the summed activity and threshold. The distributions of normalized avalanche size, avalanche duration, and the quiescent duration all exhibit hallmark features of near-critical systems (Figure 3B). More specifically, there is an approximately linear regime in the log-log plot, which then transitions at a cutoff point to a rapid decline as magnitude increases. The linear regime in the log-log plot is referred to as a power-law, wherein the frequency of observing an event is inversely proportional to its magnitude.

Changes in the slope of the power-law or cutoff point are indicative of specific shifts in the underlying dynamics. The slope of the linear portion of the size distribution was mean $\pm$ SD 1.8 $\pm$ 0.1 at baseline and was not different after ibogaine (one-way ANOVA: $F_{2,19} = 0.1190$, $p = .88$; Tukey's post hoc test for ibogaine, $p = .88$, and for saline $p = .98$). The cutoff point, on the other hand, was shifted following ibogaine (one-way ANOVA: $F_{2,19} = 10.24$, $p = .001$; Tukey's post hoc test for ibogaine, $p = .003$, and for saline $p = .92$). Under ibogaine, the network generated fewer large events despite the increase in activity rate. This indicates that the additional activity occurred outside of the large information cascade events.

The first-order avalanche statistics presented above do not provide information about the temporal relationships between bursts of neuronal activity. To quantify these relationships, we computed correlations among and between successive avalanche sizes and quiescent durations (see Supplemental Methods). Avalanches tended to be followed by avalanches of similar size in the baseline condition, and this tendency was weakened by ibogaine (Figure 3C) (RM-ANOVA: $F_{29,1189} = 10.32$, $p < .001$) but not saline (RM-ANOVA: $F_{29,1218} = 0.8484$, $p = .69$). This effect was even more striking when the autocorrelation over the past 3 and future 3 avalanches were averaged (Figure 3C, right panel). This window-averaged avalanche autocorrelation was affected by ibogaine (one-way ANOVA: $F_{2,56} = 22.94$, $p < .0001$; Tukey's post hoc test for ibogaine, $p < .0001$), but not after saline ($p = .50$). Similarly, quiescent periods of similar duration tended to follow one another in both baseline and saline conditions (Figure 3D) (RM-ANOVA: $F_{29,1218} = 1.030$, $p = .42$), but this trend was diminished by ibogaine (RM-ANOVA: $F_{29,1189} = 7.754$, $p < .0001$). This was recapitulated in the window-averaged values; ibogaine decreased the autocorrelation (one-way ANOVA: $F_{2,56} = 26.01$, $p < .0001$; Tukey's post hoc test for ibogaine, $p < .0001$), while saline did not ($p = .56$). We reliably obtained these results for many different binarizing threshold values and even when a random cell subsampling method was implemented.

The cross-correlation between avalanche sizes and subsequent quiescent times was negative, indicating that large avalanches tended to be followed by short quiescent periods, and short avalanches were followed by long quiescent times (Figure 3E). This relationship was not different between baseline and saline conditions (Figure 3E) (RM-ANOVA: $F_{60,2520} = 0.8442$, $p = .79$). In contrast, ibogaine decreased the negative correlation (RM-ANOVA: $F_{60,2460} = 9.872$, $p < .0001$). This, again, was even more striking when being averaged over the window of 3 previous and 3 future events; the cross-correlation was significantly reduced following ibogaine (main effect of injection ANOVA: $F_{2,56} = 59.77$, $p < .0001$; Tukey's post hoc test for ibogaine, $p < .0001$), but not saline ($p = .67$). In sum, the temporal extent of all tested correlations was reduced after ibogaine. Thus, it seems that ibogaine shortened the temporal window during which signals are integrated in the RSC.

DISCUSSION

In this study, the nonclassic psychedelic ibogaine destabilized the linkage between RSC neuron activity and location on a treadmill belt, which significantly reduced the ability to decode position from ensemble activity. Many RSC cells encoded positions between cues prior to ibogaine, as shown previously (8). Ibogaine administration reduced the position-related MI of individual RSC cells in the noncue regions and impaired position decoding from the population. This indicates that the RSC either cannot properly process positional information or more likely that afferent positional information is corrupted. RSC positional information depends on intact hippocampal processing (15), and hippocampal place cells have long been known to encode position in the absence of detectable landmarks, which involves using path integration to update the cognitive map (13). Therefore, the loss of positional information between landmarks in RSC may reflect ibogaine-mediated impairment of path integration and/or instability of the cognitive map. Interestingly, the cells that were activated upon traversal of the tactile cues were less affected by the drug than cells that were activated at locations between these cues. This could reflect preservation of somatosensory signals to the

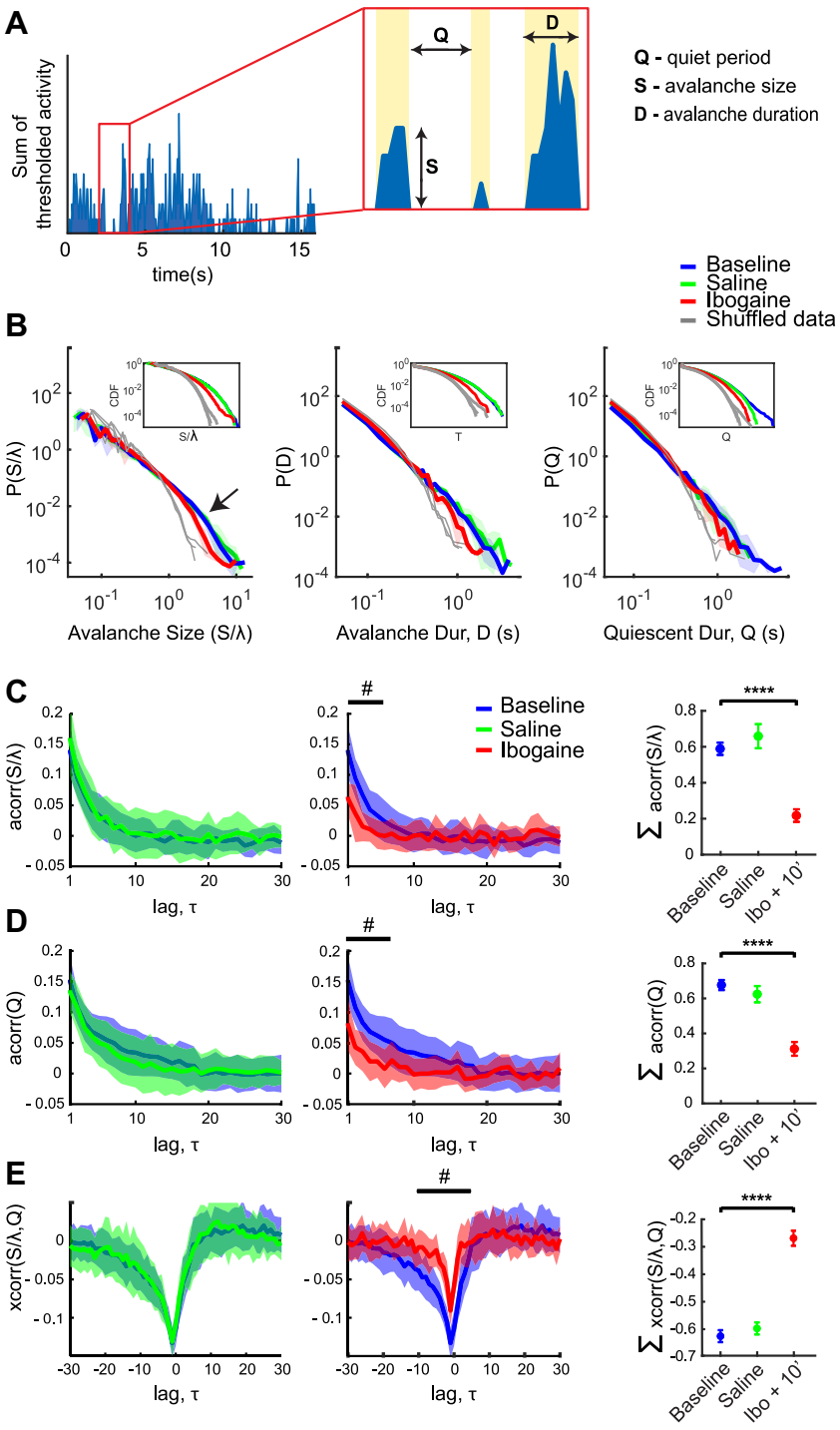

Figure 3. Neural avalanches. **(A)** Diagram showing parametrization of avalanche size, duration, and quiescent period duration from the sum of thresholded activity among simultaneously recorded cells (blue trace). Λ is a scaling factor applied to each recording prior to generating grand averages over recordings. It is the product of the number of neurons and the mean firing rate of the population in the recording. **(B)** Frequency distributions of normalized avalanche size (left panel), avalanche duration (center panel), and quiet period duration (right panel) for baseline, saline administration, and ibogaine administration. Data in all plots show mean ± 1 SD computed over all sessions of each type. The arrow indicates the cutoff point for baseline. Insets show cumulative densities from large to small values. **(C)** Correlations among the size of an avalanche and the size of future avalanches. Right-side panel shows mean and standard deviation for successive avalanches in a window including the past 3 and future 3 events. **(D)** Correlation among duration of an avalanche and the duration of future quiescent periods. **(E)** Cross-correlation of avalanche size and the duration of past/current quiescent periods. These data show that ibogaine reduced correlation structure among events, but the properties of the events themselves (e.g., power-law slope of size, duration, and quiescent periods) were not affected much. This suggests that ibogaine had little effect on the propagation of network activity within the retrosplenial cortex. #$p < .05$ (statistical significance of correlation values). ****$p < .0001$ (statistical difference of means). acorr, autocorrelation; CDF, cumulative distribution function; Ibo, ibogaine; xcorr, cross-correlation.

RSC or restabilization of the cognitive map upon traversing landmarks. The loss of spatial information under ibogaine may explain previous reports that ibogaine impairs spatial learning in rats (21).

Previous reports on the effects of psychedelic compounds on brain function have been largely based on human imaging using drugs such as psilocybin (29,36,37), lysergic acid diethylamide (5,34), and ayahuasca/DMT (38–40). The

psychedelic actions of these drugs are due to agonism of the serotonin 5-HT_{2A} receptor (41,42). In humans, these drugs generally increase the distribution of activity covariance motifs among brain regions (34,37) and promote cortical desynchronization (29,40). The data from the current study suggest similar effects at the cellular level. Note that although ibogaine agonizes 5-HT_{2A}, it has broader effects on 5-HT signaling and other neuromodulators than do classic psychedelics (43,44). We cannot rule out the possibility that these latter effects contribute to the loss of spatial information and discoordination of neural activity. If these do contribute, then the effect may not be specific to psychedelics and may also be produced by other psychoactive drugs. Correlation analysis showed that the dominant motifs were abolished by ibogaine, and the newly emergent motifs were less distinct from one another. Moreover, the explained variance of the top principal component analysis factors was reduced, indicating that the neurons became more functionally independent from one another. At least part of these effects can be explained by the deterioration of positional signaling, meaning that cells with overlapping position fields will exhibit covariation, which will be reduced by the destabilization of position fields by ibogaine. The avalanche analysis, on the other hand, is more independent of information encoding. Nonetheless, it likewise revealed a reduction in the timescale of correlations among bursting/pause events. In sum, these analyses showed a loss of structure among units and across time such that causal relationships are diminished.

A recent report of the psychedelic 2,5-dimethoxy-4-iodoamphetamine (DOI) revealed a decrease in the neuronal responses to visual stimuli in layer 2/3 of the visual cortex (45). Other features such as tuning properties and retinotopic organization were not disrupted. The authors propose that these results suggest a reduction of bottom-up sensory drive, which causes the system to rely more on top-down expectations. There are several possible explanations for the discrepancy with our finding. First, DOI is a selective 5-HT_{2A} receptor agonist, whereas ibogaine affects a wider variety of neurotransmitters, such as dopamine (46,47), serotonin (48,49), and the opioid system (50,51). Therefore, the effects of ibogaine could depend on complex interactions of these neuromodulators on neural activity. Second, the afferents to the RSC and visual cortex differ. It is possible that primary inputs to the RSC, such as the hippocampal formation or anterior cingulate region of the medial prefrontal cortex, are more affected than the primary inputs to the visual cortex.

Some recent analysis of functional connectivity in functional magnetic resonance imaging data suggests that brain networks shift toward criticality under psychedelics (34). This is based on the interaction between brain regions, whereas the current data are at the level of individual neurons within a brain structure. We found that ibogaine had surprisingly little effect on network criticality, as indicated by a lack of change in the slope of the size-frequency relationship of neural activity. This suggests that the drug did not affect the propagation of information within the RSC network much, at least in the superficial layers that were the target of the current recordings. This supports the notion that the disruption of positional encoding between landmarks arises from the loss of structured input, such as the hippocampal cognitive map, rather than from a change in RSC processing. Indeed, the ibogaine-mediated disruption is strikingly similar to the effects of hippocampal lesions on encoding of space in the RSC (15). They both degrade positional encoding when animals are between landmarks. A recent study has shown that place fields of hippocampal CA1 cells were relatively stable under high-dose lysergic acid diethylamide in a navigation task that did not require path integration (52). This supports our interpretation of the current data that it is the processes needed for path integration, either the sensory inputs or the cognitive map, that are affected by ibogaine. Regardless of the neural circuits involved, the current data are consistent with proposals that psychedelics disrupt top-down predictions about future inputs (53,54), which diminishes the inhibition of bottom-up sensory information leading to increased entropy of neural activity (29,55). Here, firing rates during cue traverses increases proportionally more than noncue regions, consistent with disinhibition, and neural activity became disordered, consistent with increased entropy.

Ibogaine somewhat reduced motivation and motoric output in the current study. Although such changes could in principle modulate the firing rates of place cells (13), no evidence suggests that they could cause the severe degradation of place encoding that was observed here. Spatial representation was not remapped as could be explained by modulation of place cell firing rates but was rather lost.

Positional signaling is widespread throughout the rodent neocortex (15,56) and may serve as a framework for associative learning to impart context (56–58). Therefore, disruption of positional signaling may have widespread effects on other sensory modalities as well as on cognitive function. Psychedelics often evoke disorientation (59), suggesting that they disrupt positional signaling. The hippocampus, in particular, has been proposed to bind together attributes of experience that are represented in the neocortex (12). Disruption of this process by psychedelic drugs could provide a mechanism that accounts for their effects on perception and discoordination of neocortical activation and should be included in revised theories.

ACKNOWLEDGMENTS AND DISCLOSURES

This work was supported by the Natural Sciences and Engineering Council of Canada (AJG, BLM, MM, JD), the New Frontiers Research Fund (AJG, JD), Alberta Innovates (MM), the Branch Out Neurological Foundation (VEI), the Beswick Fellowship (VEI), and the Canadian Institute of Health Research (BLM, MM).

VEI and AJG designed the research; VEI and IME conducted/carried out the research; MM contributed tools; VEI, DPT-C, IME, DC, and JD analyzed data; and VEI, DPT-C, BLM, and AJG wrote the manuscript.

We thank Adam Neumann for technical support and HaoRan Chang for helpful discussions.

The authors report no biomedical financial interests or potential conflicts of interest.

ARTICLE INFORMATION

From the Canadian Center for Behavioural Neuroscience, Department of Neuroscience, University of Lethbridge, Lethbridge, Alberta, Canada (VEI, DPT-C, IME, MM, BLM, AJG); Department of Physics and Astronomy, University of Calgary, Calgary, Alberta, Canada (DC, JD); and Center for the Neurobiology of Learning and Memory, University of California Irvine, Irvine, California (BLM).

VEI, DPT-C, and IME contributed equally to this work.

Address correspondence to Aaron J. Gruber, Ph.D., at aaron.gruber@uleth.ca.

Received Apr 20, 2023; revised Jul 20, 2023; accepted Jul 23, 2023.

Supplementary material cited in this article is available online at https://doi.org/10.1016/j.bpsgos.2023.07.008.

REFERENCES

1. Kobayashi Y, Amaral DG (2003): Macaque monkey retrosplenial cortex: II. Cortical afferents. J Comp Neurol 466:48–79.
2. Shibata H, Naito J (2008): Organization of anterior cingulate and frontal cortical projections to the retrosplenial cortex in the rat. J Comp Neurol 506:30–45.
3. Todd TP, Mehlman ML, Keene CS, DeAngeli NE, Bucci DJ (2016): Retrosplenial cortex is required for the retrieval of remote memory for auditory cues. Learn Mem 23:278–288.
4. Fischer LF, Mojica Soto-Albors R, Buck F, Harnett MT (2020): Representation of visual landmarks in retrosplenial cortex. eLife 9: e51458.
5. Carhart-Harris RL, Muthukumaraswamy S, Roseman L, Kaelen M, Droog W, Murphy K, *et al.* (2016): Neural correlates of the LSD experience revealed by multimodal neuroimaging. Proc Natl Acad Sci U S A 113:4853–4858.
6. Preller KH, Razi A, Zeidman P, Stämpfli P, Friston KJ, Vollenweider FX (2019): Effective connectivity changes in LSD-induced altered states of consciousness in humans. Proc Natl Acad Sci U S A 116:2743–2748.
7. Alexander AS, Nitz DA (2015): Retrosplenial cortex maps the conjunction of internal and external spaces. Nat Neurosci 18:1143–1151.
8. Mao D, Kandler S, McNaughton BL, Bonin V (2017): Sparse orthogonal population representation of spatial context in the retrosplenial cortex. Nat Commun 8:243.
9. O'Keefe J, Nadel L (1978): The Hippocampus as a Cognitive Map. Oxford: Clarendon Press.
10. Behrens TEJ, Muller TH, Whittington JCR, Mark S, Baram AB, Stachenfeld KL, Kurth-Nelson Z (2018): What is a cognitive map? Organizing knowledge for flexible behavior. Neuron 100:490–509.
11. Teyler TJ, DiScenna P (1985): The role of hippocampus in memory: A hypothesis. Neurosci Biobehav Rev 9:377–389.
12. Teyler TJ, Rudy JW (2007): The hippocampal indexing theory and episodic memory: Updating the index. Hippocampus 17:1158–1169.
13. McNaughton BL, Battaglia FP, Jensen O, Moser EI, Moser MB (2006): Path integration and the neural basis of the 'cognitive map'. Nat Rev Neurosci 7:663–678.
14. Jayakumar RP, Madhav MS, Savelli F, Blair HT, Cowan NJ, Knierim JJ (2019): Recalibration of path integration in hippocampal place cells. Nature 566:533–537.
15. Esteves IM, Chang H, Neumann AR, Sun J, Mohajerani MH, McNaughton BL (2021): Spatial information encoding across multiple neocortical regions depends on an intact hippocampus. J Neurosci 41:307–319.
16. Cooper BG, Manka TF, Mizumori SJY (2001): Finding your way in the dark: The retrosplenial cortex contributes to spatial memory and navigation without visual cues. Behav Neurosci 115:1012–1028.
17. Carhart-Harris RL, Friston KJ (2019): REBUS and the anarchic brain: Toward a unified model of the brain action of psychedelics. Pharmacol Rev 71:316–344.
18. Kohek M, Ohren M, Hornby P, Alcázar-Córcoles MÁ., Bouso JC (2020): The ibogaine experience: A qualitative study on the acute subjective effects of ibogaine. Anthropol Conscious 31:91–119.
19. Sershen H, Hashim A, Lajtha A (2001): Characterization of multiple sites of action of ibogaine. Alkaloids Chem Biol 56:115–133.
20. Rambousek L, Palenicek T, Vales K, Stuchlik A (2014): The effect of psilocin on memory acquisition, retrieval, and consolidation in the rat. Front Behav Neurosci 8:180.
21. Kesner RP, Jackson-Smith P, Henry C, Amann K (1995): Effects of ibogaine on sensory-motor function, activity, and spatial learning in rats. Pharmacol Biochem Behav 51:103–109.
22. Johnson MW, Hendricks PS, Barrett FS, Griffiths RR (2019): Classic psychedelics: An integrative review of epidemiology, therapeutics, mystical experience, and brain network function. Pharmacol Ther 197:83–102.
23. Köck P, Froelich K, Walter M, Lang U, Dürsteler KM (2022): A systematic literature review of clinical trials and therapeutic applications of ibogaine. J Subst Abuse Treat 138:108717.
24. Maxim P, Brown TI (2023): Toward an understanding of cognitive mapping ability through manipulations and measurement of schemas and stress. Top Cogn Sci 15:75–101.
25. Marton S, González B, Rodríguez-Bottero S, Miquel E, Martínez-Palma L, Pazos M, *et al.* (2019): Ibogaine administration modifies GDNF and BDNF expression in brain regions involved in mesocorticolimbic and nigral dopaminergic circuits. Front Pharmacol 10:193.
26. Blackburn JR, Szumlinski KK (1997): Ibogaine effects on sweet preference and amphetamine induced locomotion: Implications for drug addiction. Behav Brain Res 89:99–106.
27. Szumlinski KK, Haskew RE, Balogun MY, Maisonneuve IM, Glick SD (2001): Iboga compounds reverse the behavioural disinhibiting and corticosterone effects of acute methamphetamine: Implications for their antiaddictive properties. Pharmacol Biochem Behav 69:485–491.
28. Souza BC, Pavão R, Belchior H, Tort ABL (2018): On information metrics for spatial coding. Neuroscience 375:62–73.
29. Muthukumaraswamy SD, Carhart-Harris RL, Moran RJ, Brookes MJ, Williams TM, Errtizoe D, *et al.* (2013): Broadband cortical desynchronization underlies the human psychedelic state. J Neurosci 33:15171–15183.
30. Barnett L, Muthukumaraswamy SD, Carhart-Harris RL, Seth AK (2020): Decreased directed functional connectivity in the psychedelic state. NeuroImage 209:116462.
31. Beggs JM, Plenz D (2003): Neuronal avalanches in neocortical circuits. J Neurosci 23:11167–11177.
32. Lombardi F, Herrmann HJ, Plenz D, de Arcangelis L (2016): Temporal correlations in neuronal avalanche occurrence. Sci Rep 6: 24690.
33. Yaghoubi M, de Graaf T, Orlandi JG, Girotto F, Colicos MA, Davidsen J (2018): Neuronal avalanche dynamics indicates different universality classes in neuronal cultures. Sci Rep 8:3417.
34. Atasoy S, Roseman L, Kaelen M, Kringelbach ML, Deco G, Carhart-Harris RL (2017): Connectome-harmonic decomposition of human brain activity reveals dynamical repertoire re-organization under LSD. Sci Rep 7:17661.
35. Curic D, Ivan VE, Cuesta DT, Esteves IM, Mohajerani MH, Gruber AJ, Davidsen J (2021): Deconstructing scale-free neuronal avalanches: Behavioral transitions and neuronal response. J Phys Complex 2: 045010.
36. Carhart-Harris RL, Erritzoe D, Williams T, Stone JM, Reed LJ, Colasanti A, *et al.* (2012): Neural correlates of the psychedelic state as determined by fMRI studies with psilocybin. Proc Natl Acad Sci U S A 109:2138–2143.
37. Tagliazucchi E, Carhart-Harris R, Leech R, Nutt D, Chialvo DR (2014): Enhanced repertoire of brain dynamical states during the psychedelic experience. Hum Brain Mapp 35:5442–5456.
38. Alonso JF, Romero S, Mañanas MÀ., Riba J (2015): Serotonergic psychedelics temporarily modify information transfer in humans. Int J Neuropsychopharmacol 18:pyv039.
39. Palhano-Fontes F, Andrade KC, Tofoli LF, Santos AC, Crippa JA, Hallak JE, *et al.* (2015): The psychedelic state induced by ayahuasca modulates the activity and connectivity of the default mode network. PLoS One 10:e0118143.
40. Riga MS, Lladó-Pelfort L, Artigas F, Celada P (2018): The serotonin hallucinogen 5-MeO-DMT alters cortico-thalamic activity in freely moving mice: Regionally selective involvement of 5-HT1A and 5-HT2A receptors. Neuropharmacology 142:219–230.
41. Smith RL, Canton H, Barrett RJ, Sanders-Bush E (1998): Agonist properties of N,N-dimethyltryptamine at serotonin 5-HT2A and 5-HT2C receptors. Pharmacol Biochem Behav 61:323–330.

42. Madsen MK, Fisher PM, Burmester D, Dyssegaard A, Stenbæk DS, Kristiansen S, *et al.* (2019): Psychedelic effects of psilocybin correlate with serotonin 2A receptor occupancy and plasma psilocin levels. Neuropsychopharmacology 44:1328–1334.
43. Bulling S, Schicker K, Zhang YW, Steinkellner T, Stockner T, Gruber CW, *et al.* (2012): The mechanistic basis for noncompetitive ibogaine inhibition of serotonin and dopamine transporters. J Biol Chem 287:18524–18534.
44. Coleman JA, Yang D, Zhao Z, Wen PC, Yoshioka C, Tajkhorshid E, Gouaux E (2019): Serotonin transporter–ibogaine complexes illuminate mechanisms of inhibition and transport. Nature 569: 141–145.
45. Michaiel AM, Parker PRL, Niell CM (2019): A hallucinogenic serotonin-2A receptor agonist reduces visual response gain and alters temporal dynamics in mouse V1. Cell Rep 26:3475–3483.e4.
46. Maisonneuve IM, Keller RW, Glick SD (1991): Interactions between ibogaine, a potential anti-addictive agent, and morphine: An in vivo microdialysis study. Eur J Pharmacol 199:35–42.
47. Sershen H, Harsing LG, Hashim A, Lajtha A (1992): Ibogaine reduces amphetamine-induced locomotor stimulation in C57BL/6By mice, but stimulates locomotor activity in rats. Life Sci 51:1003–1011.
48. Broderick PA, Phelan FT, Eng F, Wechsler RT (1994): Ibogaine modulates cocaine responses which are altered due to environmental habituation: In vivo microvoltammetric and behavioral studies. Pharmacol Biochem Behav 49:711–728.
49. Mash DC, Staley JK, Baumann MH, Rothman RB, Hearn WL (1995): Identification of a primary metabolite of ibogaine that targets serotonin transporters and elevates serotonin. Life Sci 57:PL45–PL50.
50. Codd EE (1995): High affinity ibogaine binding to a mu opioid agonist site. Life Sci 57:PL315–PL320.
51. Glick SD, Maisonneuve IM, Pearl SM (1997): Evidence for roles of κ-opioid and NMDA receptors in the mechanism of action of ibogaine. Brain Res 749:340–343.
52. Domenico C, Haggerty D, Mou X, Ji D (2021): LSD degrades hippocampal spatial representations and suppresses hippocampal-visual cortical interactions. Cell Rep 36:109714.
53. Clark A (2013): Whatever next? Predictive brains, situated agents, and the future of cognitive science. Behav Brain Sci 36:181–204.
54. Pink-Hashkes S, Van Rooij I, Kwisthout J (2017): Perception is in the details: A predictive coding account of the psychedelic phenomenon. Presented at the 39th Annual Meeting of the Cognitive Science Society (CogSci 2017), July 26–29, London, United Kingdom.
55. Friston K (2010): The free-energy principle: A unified brain theory? Nat Rev Neurosci 11:127–138.
56. Mashhoori A, Hashemnia S, McNaughton BL, Euston DR, Gruber AJ (2018): Rat anterior cingulate cortex recalls features of remote reward locations after disfavoured reinforcements. eLife 7:e29793.
57. Gruber AJ, McDonald RJ (2012): Context, emotion, and the strategic pursuit of goals: Interactions among multiple brain systems controlling motivated behavior. Front Behav Neurosci 6:50.
58. Chang H, Esteves IM, Neumann AR, Sun J, Mohajerani MH, McNaughton BL (2020): Coordinated activities of retrosplenial ensembles during resting-state encode spatial landmarks. Philos Trans R Soc Lond B Biol Sci 375:20190228.
59. Garcia-Romeu A, Kersgaard B, Addy PH (2016): Clinical applications of hallucinogens: A review. Exp Clin Psychopharmacol 24:229–268.